UNIVERSITY OF CALIFORNIA,
IRVINE

Elucidation of Speckleplethysmography as an Alternative to Photoplethysmography for Deriving Blood Pressure

THESIS

submitted in partial satisfaction of the requirements
for the degree of

MASTER OF SCIENCE

in Computer Engineering

by

Floranne Tavailau Ellington

Thesis Committee:
Professor Hung Cao, Chair
Professor Nikil Dutt
Professor Zhou Li

2022

DEDICATION

To my parents, family, and friends who have supported me throughout my academic journey and pushed me to accomplish my goals.

TABLE OF CONTENTS

LIST OF FIGURES

LIST OF TABLES

ACKNOWLEDGMENTS

First, I would like to thank my advisor, Professor Hung Cao, who has guided and supported me through out graduate school and whom I am looking forward to continue working with to earn my PhD.

I would like to thank my labmates for their help in performing the experiments and reviewing this paper.

Additionally, I would like to thank my committee members, Professor Nikil Dutt and Professor Zhou Li, for their patience and time while being part of my master's degree journey.

Lastly, I would also like to thank the GAANN fellowship which provided me financial support to pursue my Master's Degree and focus on performing research.

ABSTRACT OF THE THESIS

Elucidation of Speckleplethysmography as an Alternative to Photoplethysmography for Deriving Blood Pressure

By

Floranne Tavailau Ellington

Master of Science in Computer Engineering

University of California, Irvine, 2022

Professor Hung Cao, Chair

Speckleplethysmography (SPG) is a recently realized biosignal to measure heart rate variability using a technique called laser speckle contrast imaging (LSCI). Compared to electrocardiography (ECG) and photoplethysmography (PPG), which are the signals used for deriving continuous non-invasive blood pressure (BP), SPG is under explored and researched, especially concerning its relationship with BP. Studies into the relationship between SPG and PPG have revealed that SPG has a higher signal to noise ratio, less sensitivity to melanin content in skin for recording, and cleaner readings in colder environments than PPG. Additionally, a clear correlation is demonstrated between the two signals not only in their nature of blood flow measurement but in their signal peaks relative to ECG. SPG has also been proven to be low cost in components to record and is able to be adapted onto mobile or wearable platforms, making it ideal for future remote and continuous systems. To demonstrate the potential for SPG to be a viable substitute for PPG in BP measurement, several experiments were conducted using a custom phone system and compared to simultaneously recorded PPG and ECG signals. From these signals, the pulse transit time (PTT) was calculated from the peak to peak time delay between the ECG waveform and the PPG and SPG signals. The PTT values from the ECG-SPG and ECG-PPG pairings were used to estimate BP and compared to a commercial gold standard device: the Omron inflatable

cuff. From the proposed experiment, SPG was able to be used as a comparable substitute for PPG in PTT based BP estimation as its results produced a similar or smaller error than the BP predicted from PPG. This experiment shows the potential to create an alternative BP system that is simple, accessible, and cost effective for users and researchers alike. To build upon the findings in this thesis, more experiments with larger datasets and different mathematical models capturing the relationship between BP and PTT will be conducted to further explore the connection between SPG and BP.

Chapter 1

Introduction

In healthcare, blood pressure (BP) measurement is an essential tool to determine the health of a patient. BP is defined into two numbers: systolic and diastolic. Systolic BP (SBP) measures the pressure in an arteries when the heart beats while diastolic BP (DBP) measures the pressure of the arteries when the heart is resting in between heart beats. A normative measurement of SBP and DBP numbers are less than 120 and 80 mmHg, respectively. High blood pressure (HBP) or hypertension, which is defined as a reading of 140 and 90 mmHg or higher, is a sign that a patient is at risk of heart attacks and strokes, two of the leading causes of death in the United States. In 2019, the Center of Disease Control and Prevention reported that hypertension was a primary or related cause of death for over half a million deaths in the United States [1]. Currently, almost half of the adults in the US have hypertension, with only 1 out of 4 actively monitoring and mitigating their HBP [1]. HBP has no visible symptoms as the only definitive method to check for HBP is measuring one's BP.

Currently, the gold standard for hospital BP measurements is catheter based arterial blood pressure (ABP); however, this requires an invasive procedure during which an applicator is inserted into a blood vessel. Thus, this method is not viable for continuous, remote

monitoring. For most commercial devices and hospital checkups, an inflatable cuff is used to determine BP. As this measures ABP too, cuff-based systems are the most accurate tool for remote and non-invasive BP. While this method is non-invasive, it is not feasible for continuous monitoring as multiple compressions over a short period of time can cause extreme discomfort. BP fluctuates rapidly during the day because of everyday activities, indicating a need for a continuous monitoring option for users without hindering their day to day life. Due to these pitfalls, there is a clear need for non-invasive and continuous BP acquisition for long term monitoring and wearability.

Many papers have explored and reviewed the use of biological based signals, such as electrocardiography (ECG) and photoplethysmography (PPG), to estimate BP from their relationships to the change of blood flow over time [7, 26, 17, 22, 27, 24, 16]. Using proper sensors, key locations on the body, and a combination of these signals, BP can be estimated in a non-invasive and potentially continuous manner, opening up a new path for BP monitoring. Researchers have investigated BP estimation using ECG and PPG and two PPG signals using a technique called pulse transit time (PTT) [4, 23, 10], but as these rely on PPG, they can be subject to error due to the shortcomings of this signal. PPG is an easy to acquire signal as the equipment is low-cost, is easy to adapt into a wearable for specific areas, such as on the wrist, finger, or earlobe, and can be recorded through reflectance or transmission mode (Fig. 1.1). However, past studies have demonstrated that PPG can have a delayed and small signal amplitude and is susceptible to low-temperature environments constricting blood vessels [6, 5, 9]. Recent papers have investigated the potential of speckleplethysmography (SPG) for heart rate variability, microvascular flow and resistance, and wearables as an alternative or replacement for PPG and illustrated how the experimental setup is also relatively inexpensive, has a higher signal to noise ratio, and can record without issue in different temperatures [5, 9, 6, 18, 20, 2]. No current literature have investigated SPG's potential as a signal in non-invasive, continuous BP monitoring. Thus, this thesis aims to help fill this gap and call attention to this area of research for future BP system

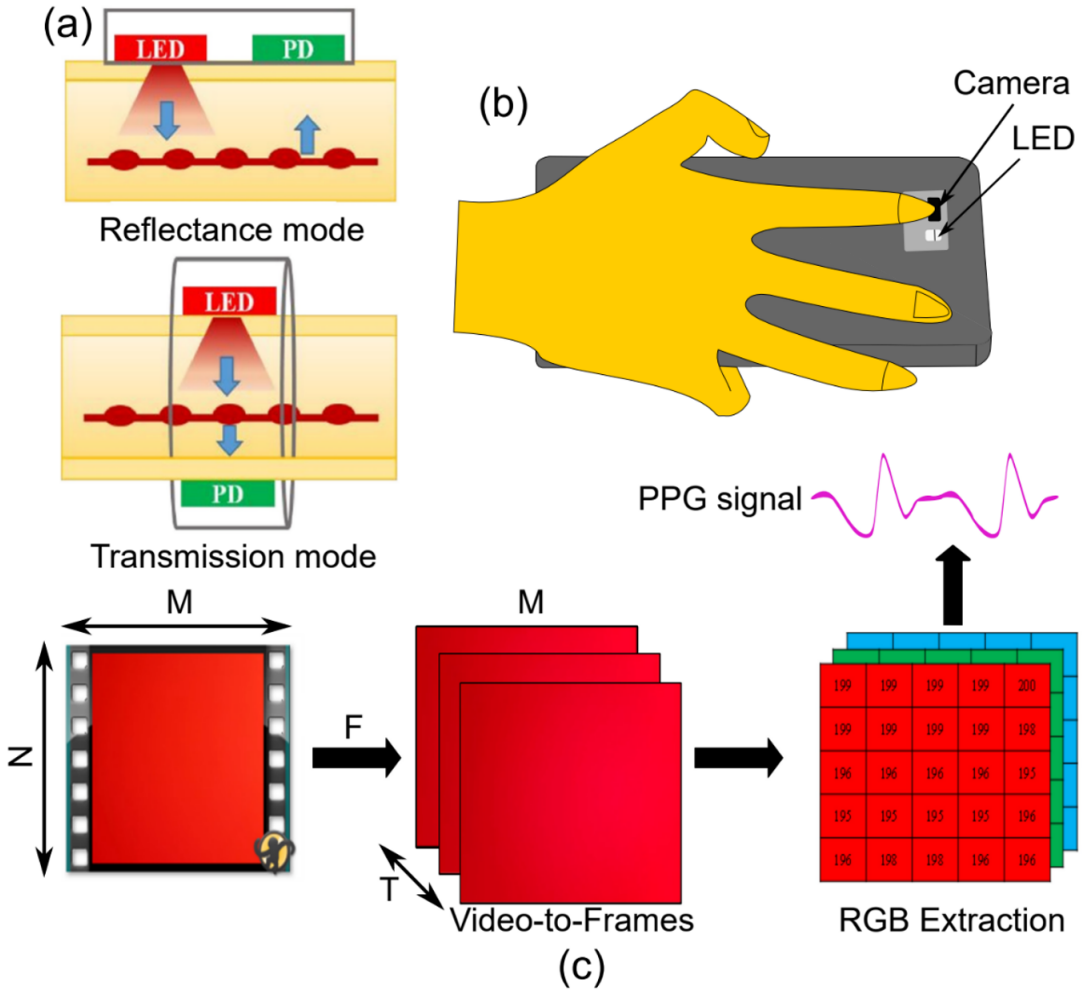

Figure 1.1: Methodology of PPG waveform acquisition:
(a) Two different modes with the use of PPG sensor: Reflectance mode and Transmission mode;
(b) A collected PPG signal with the smartphone through the camera and LED;
(c) Procedures to extract the PPG signal through a video collected by a smartphone [16]

configurations and wearable adaptations.

This study aims to explore and demonstrate the capabilities of SPG for BP measurement and its potential to replace PPG in BP PTT calculations. This paper will go over a more in-depth definition of and investigate past research findings for PTT and the three signals. Then the thesis will detail the experimental methodology, hardware and software components, and testing protocol, the results from multiple trials of the experiments, a discussion of the findings, and how this impacts the future steps for this research topic.

Chapter 2

Relevant Background and Works

In this section, current non-continuous BP measurement methods and the backgrounds of PTT, ECG, PPG, and SPG are discussed. In supplement to discussing the last three topics, related works in the field are considered to illustrate the latest research findings and the current standing of BP techniques in relation to these three signals.

2.1 Non-continuous Blood Pressure Methods

As previously stated, the gold standard in the medical field for BP measurement is using a catheter to assess ABP, which involves an invasive procedure to insert the catheter into a patient's blood vessel. As this is not feasible for long term and remote health care monitoring, an alternative ABP method has been adapted for hospital check ups and commercial BP recordings using an occluding cuff to report a static BP measurement and is comparable in BP measurements as its invasive counterpart. The occluding cuff is an improvement over catheter based ABP as it is non-invasive, quicker and simpler to perform, and adaptable to various testing environments. However, this method is still not ideal for continuous

monitoring as frequent occlusion from the cuff can cause discomfort and potentially pain to the user. Thus, many researchers have focused on alternative methods to achieve these goals for ubiquitous BP monitoring.

2.2 Pulse Transit Time and Blood Pressure

A popular method to perform BP in a continuous and non-invasive manner is to use pulse wave velocity (PWV) or, its reciprocal that this paper will be focusing on, PTT. While traveling toward the peripheral arteries, the arrival times of a pressure pulse at two different sites (i.e., proximal and distal sites) of the arterial tree are detected, which results in PTT (Fig. 2.1). This can be measured through the peak of a proximal signal and the maximum rising slope or the peak of a distal signal as well as the peak difference between two strategically placed distal signal devices. In this thesis, PTT is defined as the peak to peak difference between a proximal and distal signal for simplicity. PTT relates to BP as it demonstrates the prominence of blood flow in areas of the body over time. As PTT is the reciprocal of PWV, their features and derived equations have a high correlation to each other. The PWV parameter is determined as the ratio between the distance between the two measurement sites (D) and PTT as shown in the follow equation:

$$PWV = \frac{D}{PTT} \tag{2.1}$$

The propagation of blood in the artery is very similar to that of the propagation of a compressible fluid. The elasticity of an artery is related to the velocity of the volume pulses propagating through it, which can be described by the Moens-Kortweg equation [3]:

$$PWV = \sqrt{\frac{hE_0e^{aP}}{\rho d}} \tag{2.2}$$

where h is the thickness in an elastic artery, d is the diameter, and ρ is the blood density. E_0 is the zero-pressure modulus in mmHg, and a is a constant that depends on the particular vessel (typically 0.016 $mmHg^{-1}$ to 0.018 $mmHg^{-1}$). From equations 2.1 and 2.2, it indicates that high BP corresponds to high PWV, which in turn means a low PTT value. Many past works have used this method for BP estimation using techniques from linear regression equations to deep learning neural networks and achieved a high accuracy rate with small margins of error [4, 23, 10, 14, 17].

2.3 Electrocardiography, Photoplethysmography, and Speckleplethysmography

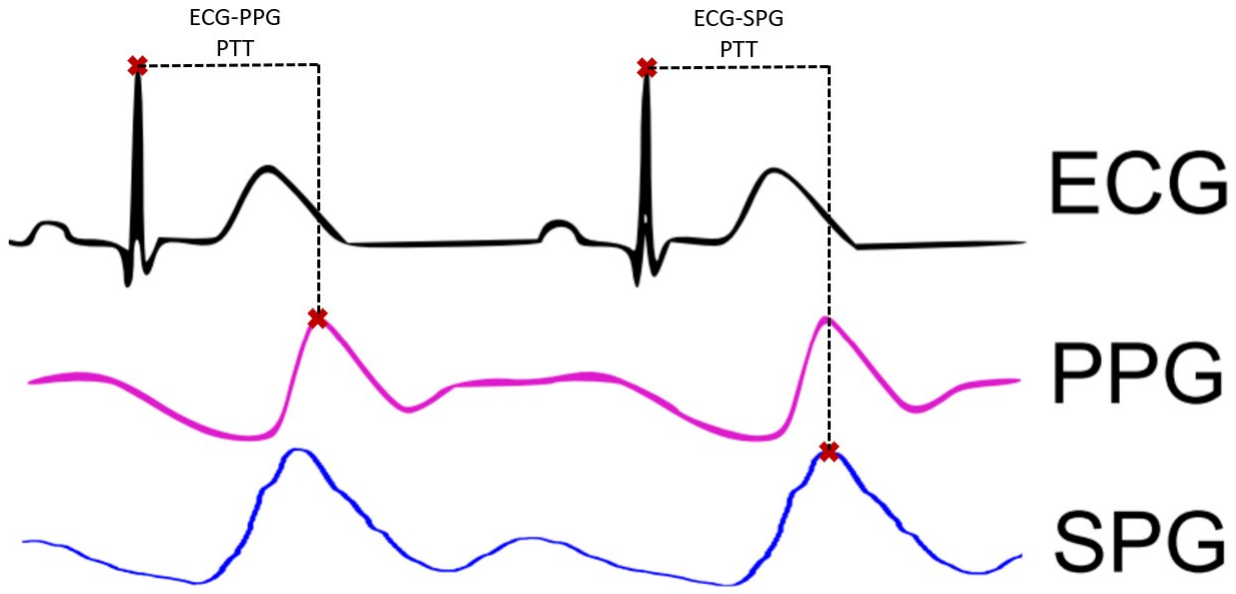

Figure 2.1: Signals demonstrating simultaneous recordings of the ECG, PPG, and SPG waveforms and how to derive PTT from ECG with either PPG or SPG

ECG is a widely used biosignal in the medical field, especially in the clinical setting, for cardiovascular-related diagnosis and vital monitoring [12]. This waveform is also a common proximal waveform used in PTT-based BP derivation and is typically paired with PPG in

cuff-less, non-invasive approaches using PTT [4, 23, 10]. This signal measures the small voltage changes in the electrical activity of the heart over time in each cardiac cycle by using electrodes attached on the body. In clinical settings, ECG electrodes are placed across the chest, lower arms, and lower legs with grounding electrodes to create a 12-lead ECG system, providing the clearest waveform [15]. This sensing technology is most commonly found in hospital and clinical settings while recently-developed approaches aim to be applicable for daily use in remote or home-based care [4, 23, 10]. Some of these home-based approaches include using 1-lead instead of 12-leads to record ECG and weaving the electrodes into textiles for signal acquisition [11, 19]. The waveform includes P waves, QRS complexes, and T waves, which provides more information about the heart than other waveforms such as PPG that usually displays one or two peaks (Fig. 2.1). Current ECG methods for BP data acquisition include those employing machine learning or deep learning combined with PTT [14, 28].

PPG is an optical measurement commonly used in pulse oximetry in clinical settings for obtaining oxygen saturation information. PPG is also a prominent distal waveform used in PTT methods. This optical technique measures the amount of blood flowing in a region of interest (ROI) through the amount of optical absorption or reflection in the optical path. In other words, PPG detects the change of blood volume through a photoelectric technique [8]. PPG sensors can be classified into two separate measurement configurations: transmission mode and reflectance mode (Fig. 1.1). In the transmission mode, the sensor setup includes a light emitted diode (LED) on one side of the tissue serving as the ROI and a photodetector (PD) on the opposite side of the tissue. In this configuration, the emitted light is transmitted through the tissue and modulated by the underlying vasculature; the modulated optical energy is then detected at the other side. In the reflectance mode, the two components (i.e., LED and PD) are on the same side of the tissue, usually on the same plane. The optical signal penetrates into the tissue, and the PD will receive the reflected light back with some fluctuations due to the tissue's absorption. While the transmission mode is mainly limited

to the earlobe, fingertip, and toe, the reflectance mode is applicable to additional locations as long as the ROI is a flat area (e.g. the forehead, forearm, supraorbital artery, under the legs, and the wrist) [17]. Since the volume and distension of the arteries can be related to the pressure in the arteries, the PPG signal produces pulse waveforms that are morphologically similar to pressure waveforms [17]. Therefore, many studies have been investigating alternative methods to estimate BP through either only PPG signal or the combination of PPG signal and other physiological signals such as ECG as previously mentioned.

SPG has been recently used as an alternative distal signal to PPG for measuring heart rate variability (HRV) [6, 9]. SPG is an optical method based on laser speckle contrast imaging (LSCI) to monitor changes in blood flow [13]. This technique is also referred to as affixed transmission speckle analysis [9]. SPG devices utilize a laser source that emits a scatter of small rays through the thickness of the tissue into a CMOS camera on the other side, similar to PPG in Fig. 1.1. The camera records a raw video with at least 30 frames per second (fps) and runs image processing techniques to identify the speckles from the laser in the red channel of each frame. To measure, the user places a finger tip in the clip-on, which further improves signal quality by reducing motion artifacts. The amount of speckles detected in the image correlates to the volume of blood present at that time point, and the change over time forms the SPG waveform. Studies comparing the signal to PPG report a higher signal to ratio to the latter in situations with more motion and colder climates [6, 9]. In terms of light exposure, SPG has not been compared to PPG in this aspect as SPG tests are currently conducted in dark rooms. Similar to PPG, SPG can be measured through smartphones as there are methods using LSCI for skin blood flow acquisition [13, 21]. Although smartphones and low-grade cameras, even with the newest models, cannot capture raw images at a fast enough rate to create a video with 30 fps, the algorithms in [13, 21] can be used on standard mp4 videos to derive SPG by adjusting the camera's parameters to have the speckles recorded shown larger than a pixel. While the HRV capabilities and its properties compared to PPG have been explored, SPG's relationship to BP and its potential

to be used as a distal waveform in PTT have not been investigated in current literature. This may be due to a lack of research for SPG in healthcare measuring or less research groups focusing on this signal.

Chapter 3

Materials and Methodology

For validating SPG's potential for BP monitoring, a simple hardware system and post-experiment software configuration was constructed to record SPG, ECG, PPG, and ABP simultaneously. The following sections detail the physical system, the signal algorithms, and experimental procedure performed for each test subject.

3.1 Hardware

To evaluate the capabilities of SPG for BP monitoring, specific hardware is necessary such as a CMOS camera and a red laser. For the scope of this project, the experiment involved recording a video using a smartphone camera (A10s Samsung smartphone rear camera) with 30 frames per second and a low cost laser diode (635NM from Quarton Inc.) shining through the subject's left pointer finger (Fig. 3.1). A smartphone camera was chosen as previous literature has proven to derive SPG adequately [13, 21]. For future iterations of this experiment, this phone based setup will be adapted into an edge device for real-time signal display and in development of a prototype remote BP system. The laser is affixed

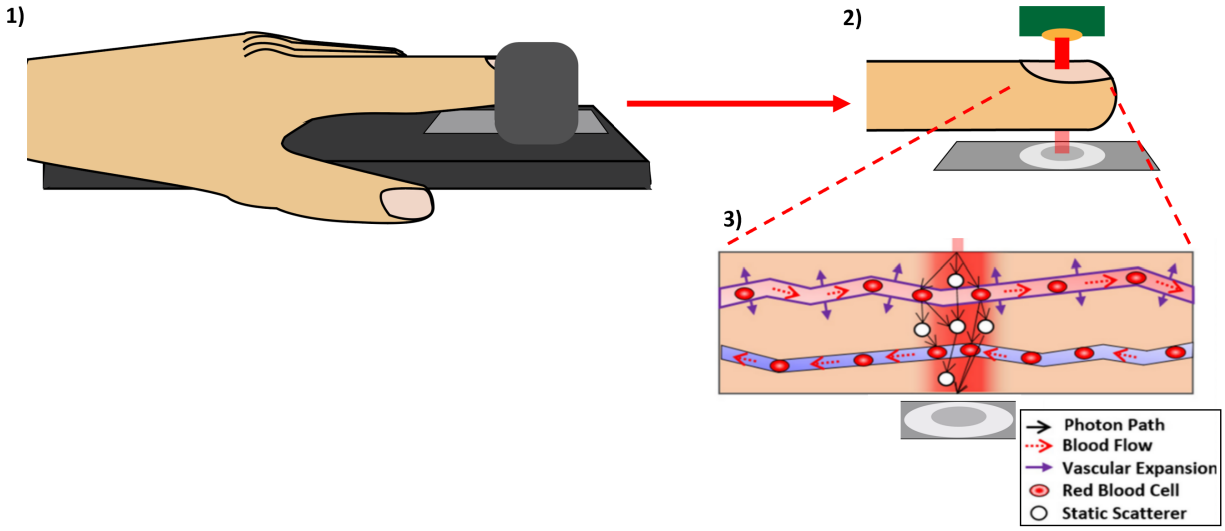

Figure 3.1: SPG System Overview. The layout of the physical device with a phone accessory holding the laser that illuminates the user's finger with the smartphone camera capturing the change over time.
1) Outside view of phone and device accessory
2) Inside view of device accessory displaying laser component shining through finger membrane to recording smartphone camera
3) Physiological view of blood vessel during SPG measuring; adapted from [6] and [16]

to the subject's finger via a Velcro strap, which allows for proper fitting between different testers, and is powered by a 3V Lithium battery (Fig. 3.2). A Bluetooth remote is connected to the smartphone to synchronize the start of the TI recording with the video recording.

For validation and comparison to previous BP monitoring methods, the AFE4950EVM Texas Instruments (TI) device reported the subjects ECG and finger PPG. This board was validated by the company as well as in this thesis author's research laboratory with other ECG and PPG devices. The ECG is measured through a 3-lead chest configuration, which is depicted in Fig. 3.3, while the PPG was recorded through the subject's left fifth digit via reflectance mode. Alongside this system, the Omron inflatable cuff was used to provide a static ABP measurement to compare and calibrate the BP value calculated from PTT.

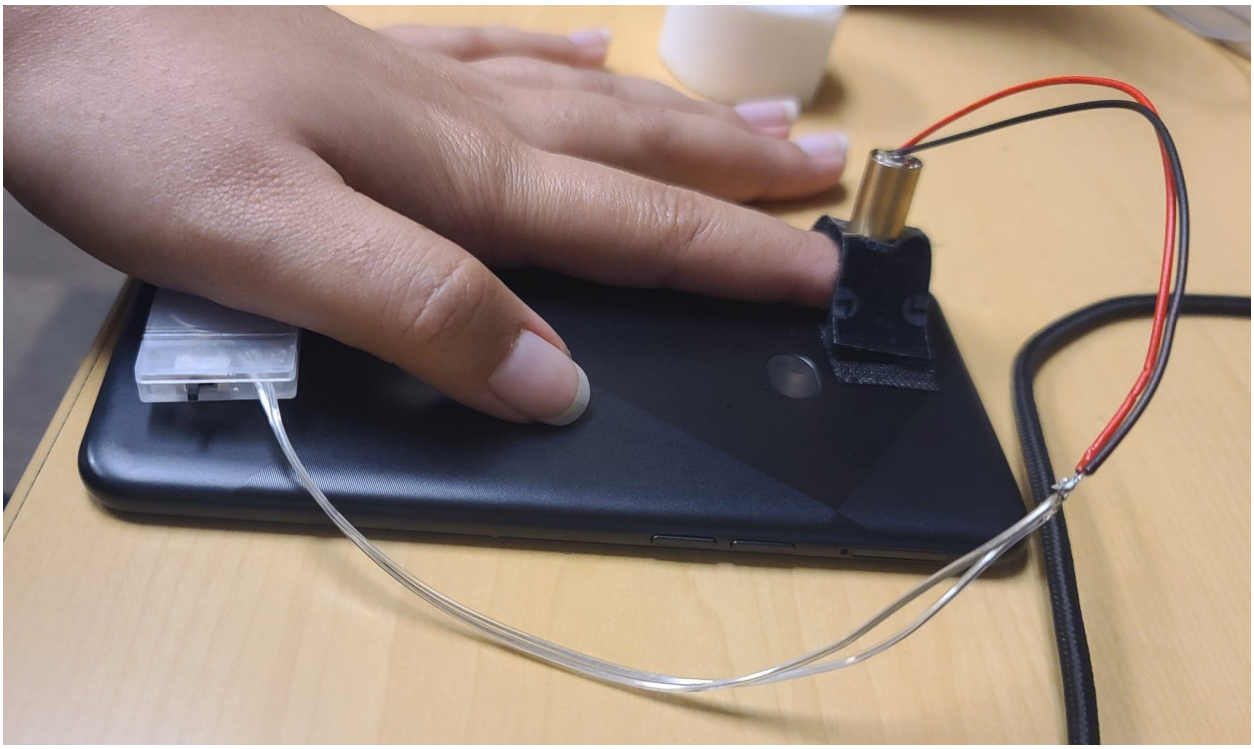

Figure 3.2: SPG Phone Configuration

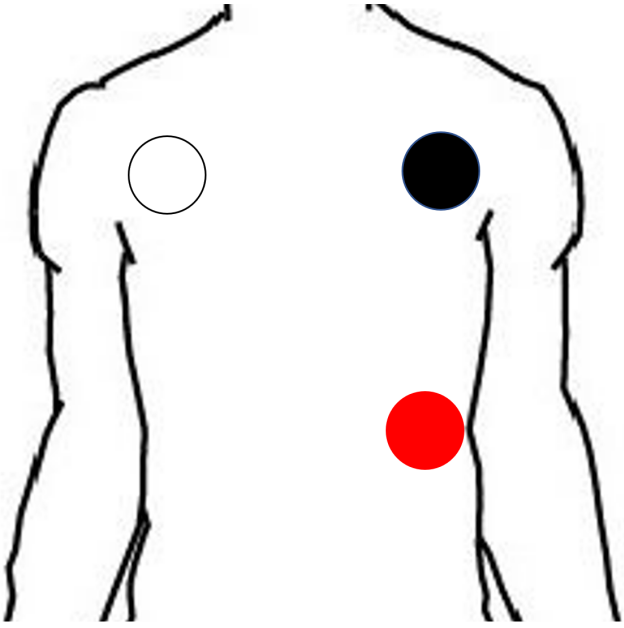

Figure 3.3: Schematic of 3-lead ECG

3.2 Software and Algorithm

To filter, display, and predict the BP from the test, a python script was written to take in an SPG video and .csv file as inputs. ECG and PPG data was exported as a .csv file from TI Bio-Signal software is adapted and sampled at 50Hz. The data was filtered to remove the wandering baseline using an open source algorithm presented in [25] and synchronized using the first clear peak of the SPG and PPG for peak comparison and PTT calculation. An additional savitzky golay filter was applied if the signal was visibly noisy. Using the video recorded through the A10e Samsung phone, the SPG was calculated from extracting the red intensity of each video frame. This value was determined through the following equation presented from [6]:

$$SPG = \frac{1}{2TK^2} \tag{3.1}$$

where T is the exposure time of the image and K is the average speckle contrast squared. The filtered ECG and PPG signal were displayed alongside the SPG signal to determine further calculations.

The peaks in each waveform were derived to use for PTT, which in this paper is defined as the peak to peak difference between the proximal and distal waveforms. The time delay between peaks between the ECG and PPG as well as ECG and PPG for PTT were ascertained for the following linear model equations:

$$BP = \frac{a}{PTT} + b \tag{3.2}$$

$$BP = \frac{a}{PTT^2} + b \tag{3.3}$$

$$BP = a \ln PTT + b \tag{3.4}$$

where a and b are the values calibrated from the static BP values line trend (Fig. 3.4), PTT is the peak to peak difference between the ECG and either the PPG or the SPG signal (Fig. 2.1), and BP is the estimated blood pressure value. The a and b values change between the 3 different stages of activity performed by the test subjects. The algorithm flow chart is depicted in Fig. 3.5.

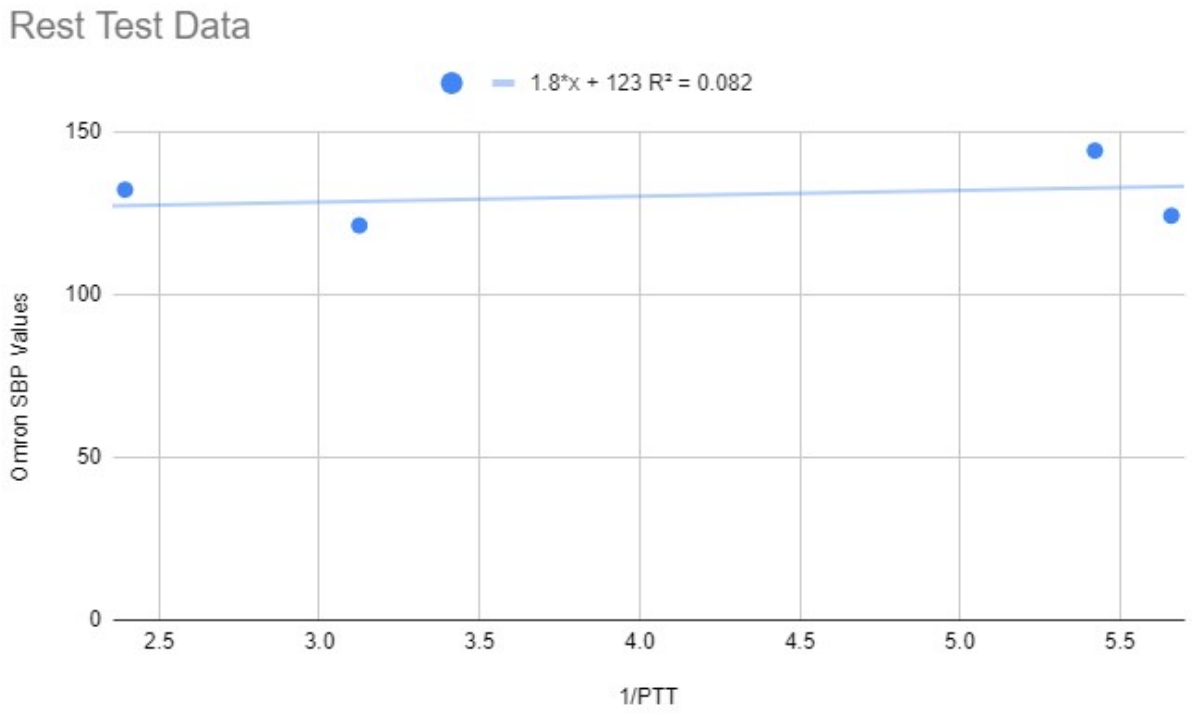

Figure 3.4: Calibration for BP estimation using the inverse of PTT and ABP values to calculate a and b for the rest test data

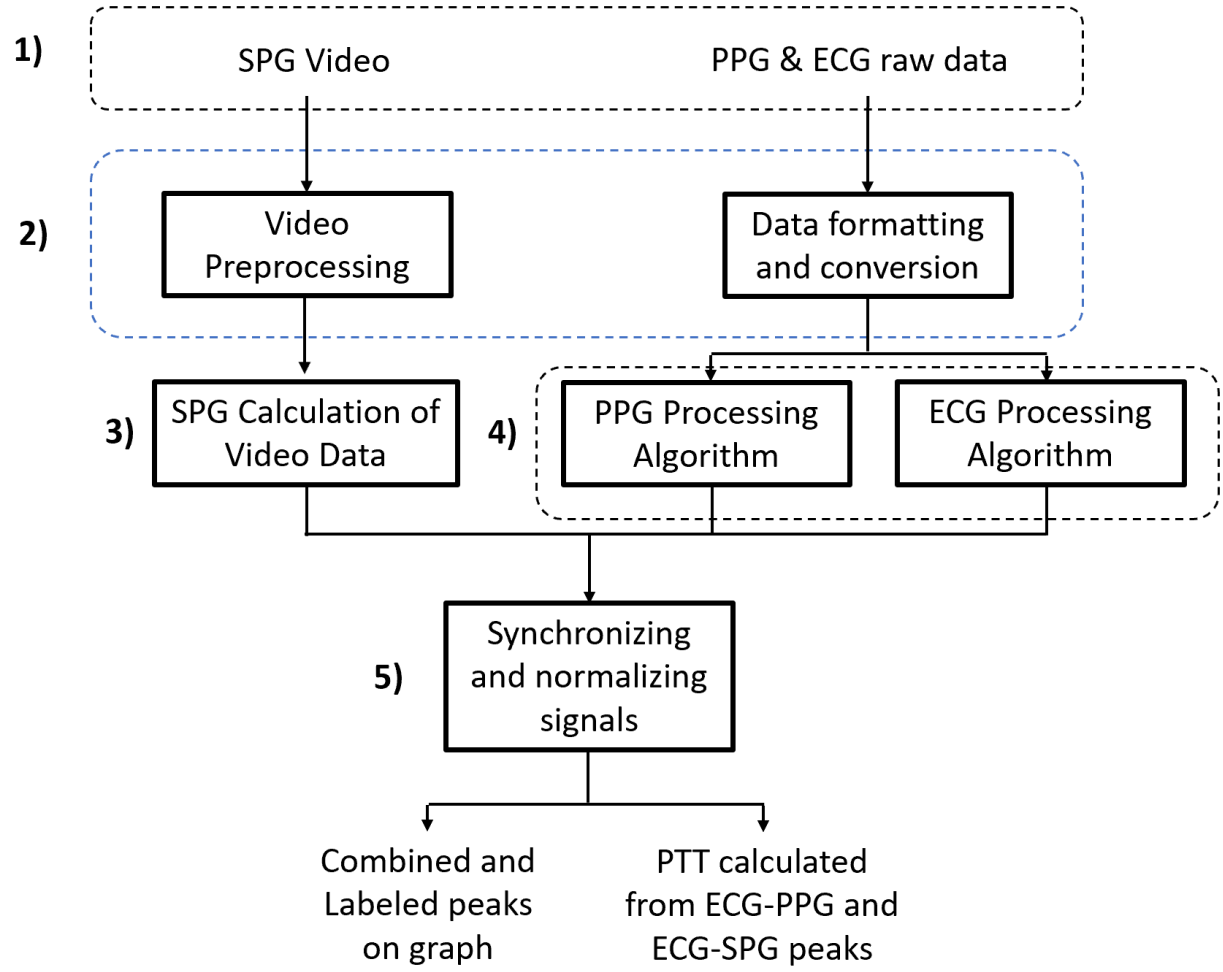

Figure 3.5: Algorithm Flow Chart for SPG, PPG, and ECG comparison.
1) Input: SPG is calculated from a short video using a smartphone camera and a simple red laser illuminating a finger. PPG and ECG are recorded using the TI AFE4950 device with the PPG sensor measuring a finger on the same hand as the SPG acquisition and ECG measured using a 3-lead configuration;
2) Preprocessing: The SPG video is converted into individual frames while the PPG and ECG data is sampled at 50Hz;
3) SPG Calculation: To determine the SPG waveform, each frame's red pixel's intensity is calculated based on the simplified speckle imaging equation 3.1;
4) PPG and ECG Processing Algorithms: The wandering baselines in the PPG and ECG signals are removed, the signal amplitudes are normalized, and an optional savitzky-golay filter is applied if the signal is visibly noisy;
5) Synchronization and Display: Using the timestamps from the input data, the SPG, PPG, and ECG waveforms are synchronized and plotted. To show the correlation between the three waveforms, the waveforms are normalized to have the same amplitude.
The output of the algorithm is a graph displaying all 3 signals and their respective labeled peaks as well as the PTT calculated between the peaks of ECG-PPG and ECG-SPG.

3.3 Experimental Procedure

The experiment can be broken into three main stages: measuring after 5 minutes of rest, after light exercise (25 jumping jacks), and after heavy exercise (walking up and down three floors of stairs). This paradigm was used to provide various BP values to fit the linear model for BP-PTT prediction. For each stage, after performing an activity, the subject's static BP using the Omron is measured from their left upper arm. Immediately after removing the cuff, the subject uses their left hand and places their fifth and second digits on the PPG and SPG sensors respectively. The ECG is measured via a 3-lead chest configuration using snap electrodes to connect the wires on the subject's chest. With the TI Bio-Sensing software and a Bluetooth controller connected to the smartphone, the signals were recorded and simultaneously started via simultaneous clicks from the test proctor. These biosignals were monitored for 60 seconds while the subject sits in a relaxed pose.

Chapter 4

Results

As previously stated in the methods chapter, the experiment was conducted in three phases with each test subject. These tests were performed on separate days as each subject's availability varied. Since many potential volunteers had prior engagements, the testing pool was limited. Each phase of the test was conducted without major delay as the only time delay between the phases was hooking up the subject to the systems. The ECG was sampled at a frequency of 500Hz and the PPG at 50Hz, which were defaults set by the TI development kit. The SPG was sampled at 30 fps as this was the highest frame rate possible with the A10e Samsung smartphone. The Omron cuff and the PPG and SPG finger readings were all performed on the subject's left arm to keep the test process standardized. The ECG was recorded from the 3-lead configuration discussed in the previous chapter with snap electrodes that the subject kept on for the total duration of the activities and tests.

From the four test subjects, the Omron SBP measurements were considered for further calculations. These values, as depicted in Table 4.1, varied between each subject due to fitness level, age, and sex. The trend of increased SBP did not uniformly occur for each test subject after each increasing level of activity. The mean from these Omron SBP values were

	Systolic Blood Pressure			
Activity	**Subject 1**	**Subject 2**	**Subject 3**	**Subject 4**
after rest	121	144	124	132
after light exercise	117	150	135	133
after heavy exercise	124	149	141	144

Table 4.1: Systolic BP reported for each subject after each key exercise

determined as well as the BP values estimated from equations 3.2, 3.3, and 3.4 using either the PTT obtained from ECG-PPG or ECG-SPG. The reported numbers were separated based on the activity performed before the signals were recorded (see Table 4.2). To further analyze the metrics presented in Table 4.2, the error percentages of the standard deviations compared to the mean SBP values were calculated for each equation and PTT pairing (see Table 4.3). As the resulting error percentages were below 10%, they were acceptable due to the small sample pool used to derive the results. The filtered signals from the proposed system demonstrated a first peak of ECG, a second following peak of SPG, and a slightly delayed final peak of PPG for each heart beat, which was expected and coincided with previous literature findings. As some parts of the signals were noisier due to motion artifacts, specific segments of the signals were used to measure PTT to derive the best values for the linear models, which are depicted in the following figures (Fig. 4.1, 4.2, 4.3). Each of these figures illustrates the resulting signals from different subjects after performing resting, light exercise, and heavy exercise.

		SD for BP from ECG-PPG PTT			SD for BP from ECG-SPG PTT		
Activity	**Mean SBP**	**1/PTT**	**1/PTTˆ2**	**ln(PTT)**	**1/PTT**	**1/PTTˆ2**	**ln(PTT)**
after rest	130.25	±8.18653	±8.13251	±8.24167	±7.36285	±7.28186	±7.34235
after light exercise	133.75	±8.62369	±8.03936	±9.13630	±8.81543	±8.65061	±8.38916
after heavy exercise	139.5	±7.80216	±7.55895	±7.90282	±5.49009	±4.57306	±6.57019

Table 4.2: Mean of the Systolic BP from the Omron cuff and the Standard Deviations of the BP values estimated from the ECG-PPG and ECG-SPG PTT values

Activity	**PPG 1/PTT**	**PPG 1/PTTˆ2**	**PPG ln(PTT)**	**SPG 1/PTT**	**SPG 1/PTTˆ2**	**SPG ln(PTT)**
after rest	6.29%	6.24%	6.32%	5.65%	5.59%	5.64%
after light exercise	6.45%	6.01%	6.83%	6.59%	6.47%	6.27%
after heavy exercise	5.59%	5.41%	5.67%	3.94%	3.28%	4.71%

Table 4.3: Error Percentages of BP estimation from each equation and PTT pairing to quantify the accuracy of SPG versus PPG

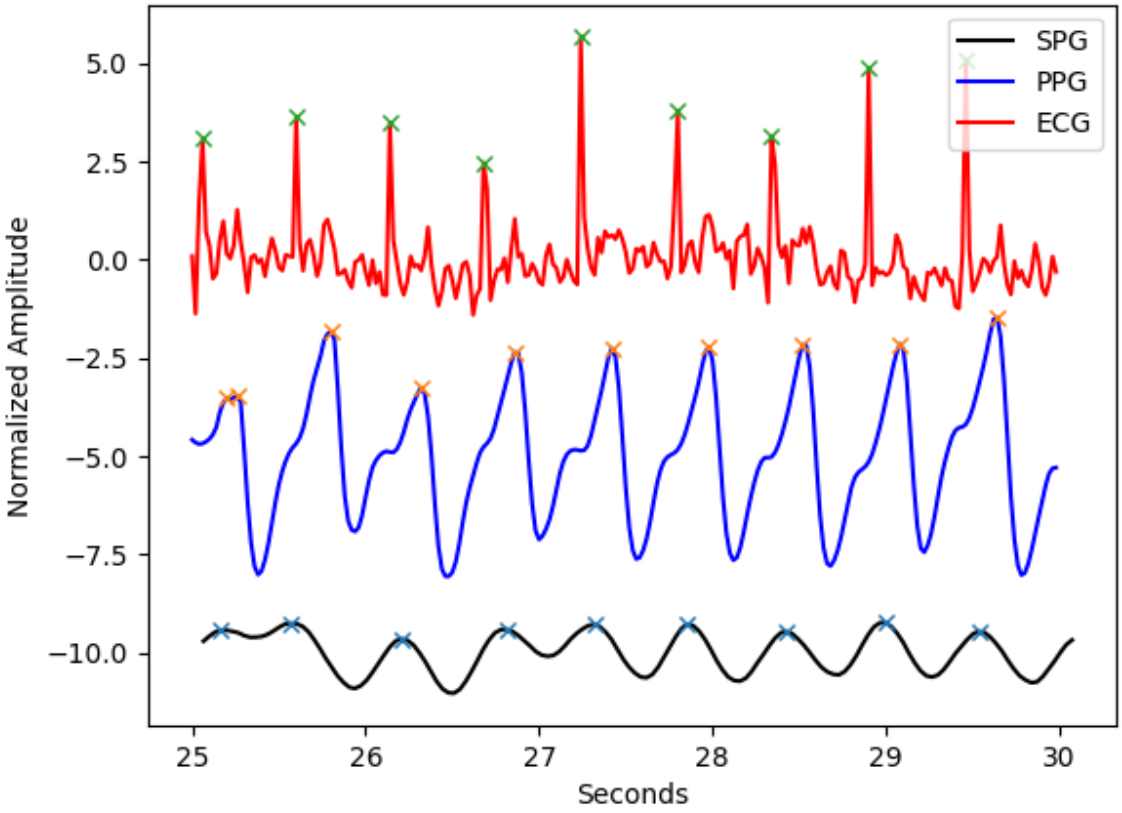

Figure 4.1: Graph output snippet displaying the three filtered signals and their detected peaks after subject was resting.

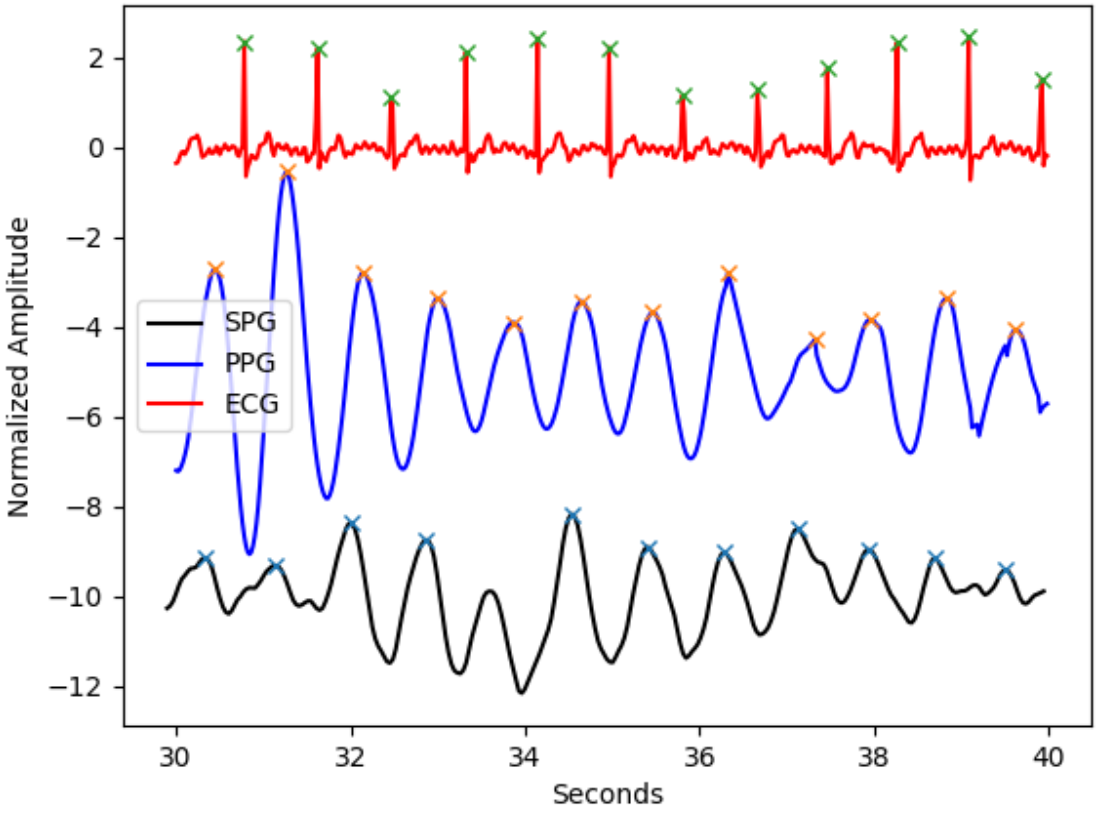

Figure 4.2: Graph output snippet displaying the three filtered signals and their detected peaks after subject was performing light exercise.

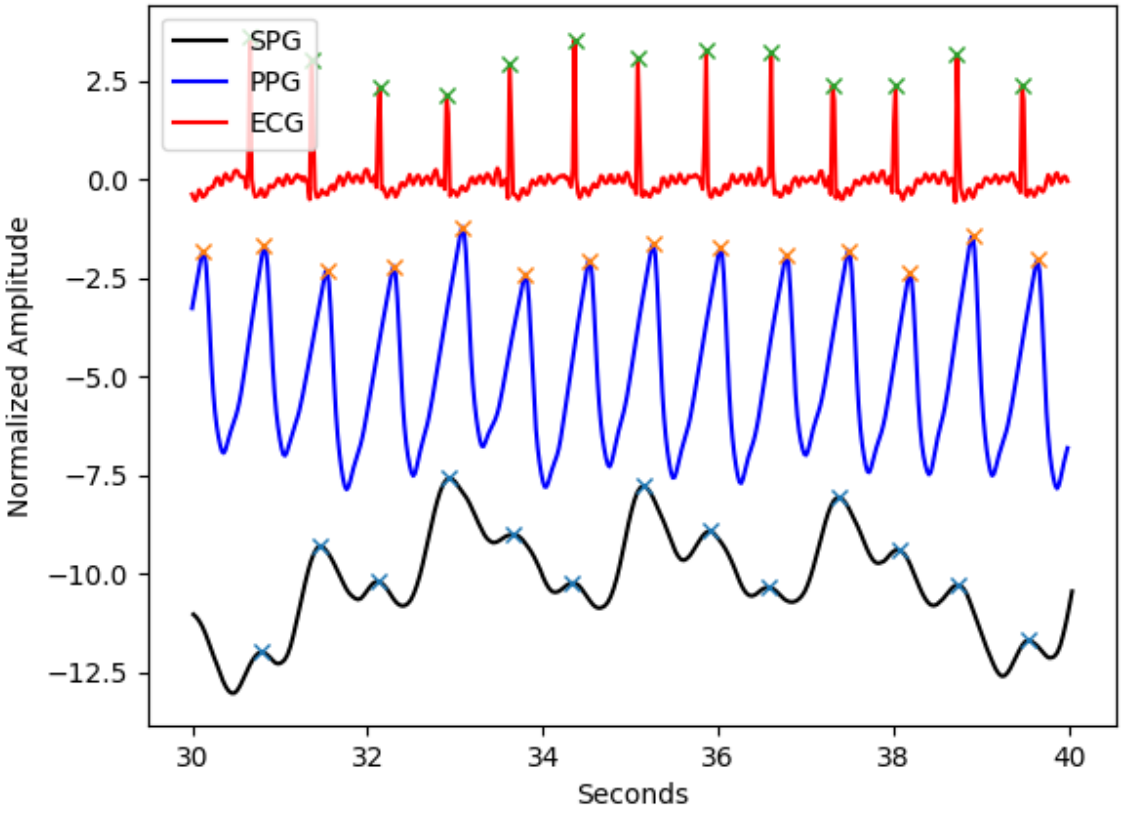

Figure 4.3: Graph output snippet displaying the three filtered signals and their detected peaks after subject was performing heavy exercise.

Chapter 5

Discussion

The experiment proposed in this thesis demonstrates that SPG has potential to be used as a substitute or replacement for PPG in PTT-based BP estimation. The first recorded trial was ultimately not used as the two separate systems for the SPG and ECG/PPG devices were not properly synchronized. This was revealed when looking at the waveforms alongside each other and seeing the SPG signal peak before the ECG signal, which is physiologically impossible as the ECG is recorded on the chest and the SPG is measured from a finger. The result of this initial trial helped refine the testing protocol, and a Bluetooth remote was introduced to the experimental configuration to solve this issue. When looking at the subsequent test data after this change, this issue was resolved and those experiments were used for data. For better comparison between the ECG and PPG signal, the ECG signal was downsampled to 50Hz. Unfortunately, when the ECG and PPG were downsampled to match the SPG signal frequency, the two signals lost key information to determine their peaks accurately. As they were all recorded versus a time domain, the signals were able to be synchronized based on the timestamps despite their varying sampling frequencies.

From applying the three linear equations, BP was estimated using the peak to peak time

delay from ECG and PPG and compared to the BP values derived from the PTT established from the ECG and SPG signal peaks. The standard deviations of the predicted results versus the mean of the SBP recorded from the test protocol's gold standard show that in the cases of recording after the light exercise, the PPG and SPG based results were comparable. Recordings performed after the first and last activities reported that SPG demonstrated higher accuracy and a smaller standard deviation (Table 4.2) compared to PPG. Table 4.3 depicts that for all three equations and the two PTT values, the error was below 7%. SPG was able to more accurately predict the SBP value than PPG by as much as 1% for resting and 1.5% after heavy exercise, which can be contributed to its earlier peak detection. As previously discussed in PTT calculations in chapter 2, a lower PTT value results in a higher BP value, a finding which was evident in the data trend. While SPG did not outperform PPG after the light exercise, the signal produced a PTT that accurately predicted within a 0.5% of PPG based PTT for each of the mathematical models. This discrepancy of SPG's accuracy may be due to the low sample pool and the light exercise not impacting BP as much as resting or heavy exercise. Another contributing feature with inaccuracy was that SBP for each subject did not linearly increase as the level of activity grew (Table 4.1), which was unexpected and not the original goal of the test protocol. This nonlinearity led to poor calibration for the equations and impacted the BP estimations, which led to a large majority of higher error percentages for both PPG and SPG versus predictions for the other two activities. A different exercise regimen for future experiments may correct this issue and consequently improve SPG based BP estimation accuracy.

As the error was below 7% for every predicted value, this demonstrated that these three mathematical models were able to adequately illustrate the relationship between BP and PTT, especially using the inverse of PTT and the inverse of the square of PTT. However, the estimations derived from the equations differed between patients and activities performed before recording. As these are linear equations, they may not fully capture how complex the human body is and how many physiological features may contribute to determining BP.

Shown from the previously discussed issue with the light exercise SBP results, the decrease in SBP versus the first activity's values was not properly accounted for by these equations. Additionally, this discrepancy may be due to the low sampling pool used for calibration, the individual health and biological differences between the subjects, and the synchronization of the SPG system and the ECG/PPG board. A larger test pool and different system format for synchronizing the two signals may produce a lower error in future iterations of this experiment.

As the SPG based results performed similarly or more precisely compared to PPG, a signal which has been explored extensively in previous literature, SPG exhibits the ability to be used in PTT based BP measurements in place of PPG. As SPG can be recorded through a low-grade CMOS camera and laser pointer, the potential for a wearable platform is possible. The signal has shown to be obtainable from a smartphone camera and laser attachment, which also exemplifies its potential to move onto a solely smartphone platform for acquisition and computation. Furthermore, since SPG is able to be recorded in transmission or reflectance mode similarly to PPG, deriving BP from two SPG placed in key ROI like past PPG experiments may be possible.

Chapter 6

Conclusion

As BP is a major tool in determining various health conditions such as hypertension, heart attacks, and strokes, having continuous, non-invasive, and remote devices is important to improve healthcare. SPG is a relatively new and unexplored biosignal, especially in the realm of BP estimation. As past literature has investigated its relationship to ECG and PPG, two prominent signals used in estimating SBP and DBP from PTT based methods, the adaption of and research into SPG for the field of BP is a logical step. From the experimental protocol described and performed in this thesis, SPG demonstrated to have interchangeable capabilities with PPG in being the distal waveform paired with ECG as the proximal waveform for PTT based BP estimation. This was determined through the similar or lower error percentages in BP estimations between PPG and SPG based PTT calculations reported by the study. Collecting more datasets and investigating various mathematical models between BP and PTT can help improve BP estimation using SPG as well as reveal more about SPG's capabilities as a distal signal. Additionally, as SPG can be obtained using low cost equipment and on a smartphone platform, the possibility for SPG to be obtained and processed on a wearable or mobile format is highly probable. As ECG and PPG have increasingly become incorporated into wearable formats, a system incorporating two or all

three signals for continuous and non-invasive BP can be developed. This would allow for more accessibility for continuous BP in remote healthcare and for integration into larger, complex monitoring systems. For the next steps of this project, a wearable, edge computation platform will be developed for future testing to further explore SPG's relationship to BP. If this investigation goes well, this signal will be integrated into a maternal and fetal healthcare system to monitor the mother's BP in relation to daily activities.

Bibliography

[1] Facts about hypertension, 09 2021.

[2] R. Bi, Y. Du, G. Singh, J.-H. Ho, S. Zhang, A. B. Ebrahim Attia, X. Li, and M. C. Olivo. Fast pulsatile blood flow measurement in deep tissue through a multimode detection fiber. *Journal of Biomedical Optics*, 25(05), 05 2020.

[3] J. C. Bramwell and A. V. Hill. The velocity of pulse wave in man. *Proceedings of the Royal Society of London. Series B, Containing Papers of a Biological Character*, 04 1922.

[4] F. S. Cattivelli and H. Garudadri. Noninvasive cuffless estimation of blood pressure from pulse arrival time and heart rate with adaptive calibration. *2009 Sixth International Workshop on Wearable and Implantable Body Sensor Networks*, 2009.

[5] C. E. Dunn, B. Lertsakdadet, C. Crouzet, A. Bahani, and B. Choi. Comparison of speckleplethysmographic (spg) and photoplethysmographic (ppg) imaging by monte carlo simulations and in vivo measurements. *Biomedical Optics Express*, 9(9), 09 2018.

[6] C. E. Dunn, D. C. Monroe, C. Crouzet, J. W. Hicks, and B. Choi. Speckleplethysmographic (spg) estimation of heart rate variability during an orthostatic challenge. *Scientific Reports*, 9(1), 10 2019.

[7] C. El-Hajj and P. Kyriacou. A review of machine learning techniques in photoplethysmography for the non-invasive cuff-less measurement of blood pressure. *Biomedical Signal Processing and Control*, 58, 01 2020.

[8] M. Elgendi, R. Fletcher, Y. Liang, N. Howard, N. H. Lovell, D. Abbott, K. Lim, and R. Ward. The use of photoplethysmography for assessing hypertension. *npj Digital Medicine*, 2(1), 06 2019.

[9] M. Ghijsen, T. B. Rice, B. Yang, S. M. White, and B. J. Tromberg. Wearable speckle plethysmography (spg) for characterizing microvascular flow and resistance. *Biomedical Optics Express*, 9(8), 07 2018.

[10] S. Ghosh, A. Banerjee, N. Ray, P. W. Wood, P. Boulanger, and R. Padwal. Continuous blood pressure prediction from pulse transit time using ecg and ppg signals. *2016 IEEE Healthcare Innovation Point-Of-Care Technologies Conference (HI-POCT)*, 2016.

[11] M. W. Gifari, H. Zakaria, and R. Mengko. Design of ecg homecare:12-lead ecg acquisition using single channel ecg device developed on ad8232 analog front end. *2015 International Conference on Electrical Engineering and Informatics (ICEEI)*, 2015.

[12] A. L. Goldberger, Z. D. Goldberger, and A. Shvilkin. *Clinical electrocardiography: a simplified approach e-book*. Elsevier Health Sciences, 2017.

[13] D. Jakovels, I. Saknite, G. Krievina, J. Zaharans, and J. Spigulis. Mobile phone based laser speckle contrast imager for assessment of skin blood flow. *SPIE Proceedings*, 10 2014.

[14] M. Kachuee, M. M. Kiani, H. Mohammadzade, and M. Shabany. Cuffless blood pressure estimation algorithms for continuous health-care monitoring. *IEEE Transactions on Biomedical Engineering*, 64(4):859–869, 2017.

[15] T. Le, I. Clark, J. Fortunato, M. Sharma, X. Xu, T. K. Hsiai, and H. Cao. Electrocardiogram: Acquisition and analysis for biological investigations and health monitoring. *Interfacing Bioelectronics and Biomedical Sensing*, page 117–142, 2020.

[16] T. Le, F. Ellington, T.-Y. Lee, K. Vo, M. Khine, S. K. Krishnan, N. Dutt, and H. Cao. Continuous non-invasive blood pressure monitoring: A methodological review on measurement techniques. *IEEE Access*, 8:212478–212498, 10 2020.

[17] R. Mukkamala, J.-O. Hahn, O. T. Inan, L. K. Mestha, C.-S. Kim, H. Toreyin, and S. Kyal. Toward ubiquitous blood pressure monitoring via pulse transit time: Theory and practice. *IEEE Transactions on Biomedical Engineering*, 62(8):1879–1901, 08 2015.

[18] J. H. Olazabal, F. Wieringa, E. Hermeling, and C. Van Hoof. Beat-to-beat intervals of speckle amp; intensity-based optical plethysmograms compared to electrocardiogram. *2021 Computing in Cardiology (CinC)*, 09 2021.

[19] D. Pani, A. Dessi, J. F. Saenz-Cogollo, G. Barabino, B. Fraboni, and A. Bonfiglio. Fully textile, pedot:pss based electrodes for wearable ecg monitoring systems. *IEEE Transactions on Biomedical Engineering*, 63(3):540–549, 2016.

[20] T. B. Rice, B. Yang, and S. White. Effect of skin optical absorption on speckleplethysmographic (spg) signals. *Biomedical Optics Express*, 11(9), 08 2020.

[21] L. M. Richards, S. M. Kazmi, J. L. Davis, K. E. Olin, and A. K. Dunn. Low-cost laser speckle contrast imaging of blood flow using a webcam. *Biomedical Optics Express*, 4(10), 09 2013.

[22] M. Sharma, K. Barbosa, V. Ho, D. Griggs, T. Ghirmai, S. Krishnan, T. Hsiai, J.-C. Chiao, and H. Cao. Cuff-less and continuous blood pressure monitoring: A methodological review. *Technologies*, 5(2), 05 2017.

[23] R. Shriram, A. Wakankar, N. Daimiwal, and D. Ramdasi. Continuous cuffless blood pressure monitoring based on ptt. *2010 International Conference on Bioinformatics and Biomedical Technology*, 2010.

[24] J. Solà and R. Delgado-Gonzalo. *Handbook of cuffless blood pressure monitoring: A practical guide for clinicians*. Springer Nature, 2020.

[25] spebern. Baseline wander removal with wavelet transform. `https://github.com/spebern/py-bwr`, 2019.

[26] A. Stojanova, S. Koceski, and N. Koceska. Continuous blood pressure monitoring as a basis for ambient assisted living (aal) – review of methodologies and devices. *Journal of Medical Systems*, 43(2), 01 2019.

[27] G. Wang, M. Atef, and Y. Lian. Towards a continuous non-invasive cuffless blood pressure monitoring system using ppg: Systems and circuits review. *IEEE Circuits and Systems Magazine*, 18(3):6–26, 08 2018.

[28] Q. Zhang, D. Zhou, and X. Zeng. Highly wearable cuff-less blood pressure and heart rate monitoring with single-arm electrocardiogram and photoplethysmogram signals. *BioMedical Engineering OnLine*, 16(1), 02 2017.